

## CHAPTER 2

### INTRODUCTION TO THE WSR-88D

**2.1 General.** The WSR-88D is the second-generation, operational meteorological radar replacing the non-Doppler meteorological radars of the National Weather Service and the Air Force.

The WSR-88D represents a quantum leap from the earlier meteorological radars both in engineering technology and in meteorological measurements. As a fully coherent "Doppler" radar, it provides not only accurate reflectivity measurement and its attendant information on spatial location, distribution, etc., but also measurement of the radial component of motion (mean Doppler velocity along the axis of the radar beam) of the scatterers and the dispersion of velocities in the radar sample volume (spectrum width). The information flow rate from the WSR-88D is an order of magnitude larger than the earlier incoherent radars and requires high-speed data processing for signal analysis and information extraction for effective utilization and man-machine interface.

**2.2 Basic Unit Description.** For descriptive purposes the WSR-88D unit can be divided into three parts.

- Radar - composed of transmitter, receiver, antenna and the associated support circuitry.
- Dedicated Signal Processors - composed of reflectivity, velocity, and spectrum width estimators; ground clutter cancellers; and data formatting, quality checking, and radar control processors.
- Data Analysis and Display - composed of the meteorological analysis processor, product generator, associated color displays, and communications ports.

The radar is a coherent "chain-transmitter" design. Coherence, or phase information, in this type of design is maintained by very stable oscillators or signal sources that operate continuously. These sources are used as the reference in extracting the Doppler shift of the return signal, which is proportional to the radial motion of the target from which the transmitter signal is backscattered. A chain transmitter is one in which the transmitter signal is initially generated at a low power level, in this case a few hundred milliwatts, and increased to a high power, 750 kilowatts (kw), by an amplifier chain. Intermediate amplification is by solid-state devices and the final high-power amplifier is a klystron. The klystron is a vacuum tube device capable of high gain amplification (~60 dB) with negligible signal distortion or spurious emission. The antenna is a center-feed, parabolic reflector having a diameter of approximately 28 ft (8.5 m). The antenna has a main lobe one-way 3 dB beam width of 0.93° at 2850 MHz (measured average), a first sidelobe level of 29 dB below the main lobe, a sidelobe taper greater than 1 dB per degree between 2° and 10° from the main lobe axis, and a far out sidelobe level more than 40 dB below the main lobe. The receiver uses two frequency mixers to down convert the received signal to zero frequency carrier (video

signal). The first conversion generates an intermediate signal carrier at which most amplification, bandpass filtering, and automatic gain control (AGC) are done. The second frequency conversion is a synchronous detection (a detection that retains received signal amplitude and phase shift difference between received and transmitted signal phases but which removes the intermediate frequency carrier). At this point, the signal has an amplitude proportional to echo radar reflectivity and contains a frequency component equal to the Doppler shift. This is a "complex" signal; complex meaning that it contains both amplitude and phase information and, for convenience of handling and analysis, is decomposed into its vector components, i.e., two signals, inphase and quadrature, having a phase difference of  $90^\circ$  that, when added vectorally, form the complex signal.

The signal processors extract three meteorological quantities from the returned signal. These are: volume reflectivity, expressed in terms of equivalent radar reflectivity,  $Z_e$ ; the radial velocity, i.e., the component of motion of the reflecting particles toward or away from the radar; and spectrum width, which is a measure of dispersion of velocities within the radar sample volume. Reflectivity,  $Z$ , is calculated from the returned signal power and the known characteristics of the radar (Appendix A.4.1). Estimation is by a linear average of several return pulses, usually about 25, from each range cell. Velocity,  $v$ , is also estimated from several pulses (usually 40 to 50) pulses. The mathematical quantity computed is the return signal complex covariance argument using a technique called "pulse-pair processing" since the computation requires two pulses (two consecutive signal returns from the same target; Appendix A.4.2). Physically, the covariance argument provides a measurement of rotation rate of the complex vector representing the returned signal that is directly related to the Doppler frequency, Spectrum width,  $W$ , or velocity dispersion within the radar sample volume, is estimated indirectly. The computation performed is the returned signal autocorrelation which is related to the velocity spectrum standard deviation. It uses the same pulses as radial velocity (Appendix A.4.3). These quantities are calculated by dedicated digital processors, i.e., processors designed and configured to perform a specific operation with only limited changes in parametric values.

Physically the WSR-88D is divided into three functional components: RDA, RPG, and display systems. These components are described in Part D of this Handbook.

**2.3 WSR-88D Radar Characteristics.** A tabulation of some of the fundamental engineering characteristics of the radar is given in Table 2-1. The implications of these values in the meteorological measurements are discussed in Chapter 3. These system parameters, when substituted into the general radar equation (Eq. 5-3 and Appendix A), result in the detection capability shown in Figure 2-1.

**Table 2-1**  
**WSR-88D Radar Characteristics**

Antenna Subsystem		
Radome	Rigid fiberglass	
Diameter	39 ft (12 meters)	
RF loss - two way	0.24 dB at 2850 MHz	
Pedestal	Elevation Over Azimuth	
	Azimuth	Elevation
Steerability	360°	+0.5 to +19.5
Rotational rate - maximum	30° s <sup>-1</sup>	30° s <sup>-1</sup>
Acceleration - maximum	15° s <sup>-2</sup>	15° s <sup>-2</sup>
Mechanical limits	-1° to +60°	
Antenna	Paraboloid of Revolution	
Polarization	Linear Horizontal	
Reflector diameter	28 ft (8.5 meters)	
Gain (at 2800 MHz)	45 dB	
Beam Width	0.93° (at 2850 MHz, Measured Average)	
First sidelobe level	-29 dB	
Transmitter and Receiver Subsystem Coherent - Chain Design		
Transmitter		
Frequency range	2700 MHz to 3000 MHz	
Peak power	750 kw	
Pulse widths (nominal)	1.57 μs and 4.5 μs	
rf duty cycle	0.002 maximum	
PRFs	Short pulse: 318 Hz to 1304 Hz	
	Long pulse: 318 Hz to 452 Hz	
Receiver		
Dynamic range	93 dB	
Noise temperature	450° K	
Intermediate frequency	57.6 MHz	
Band width, 3 dB	0.63 MHz	

<b>Table 2-1</b> <b>WSR-88D Radar Characteristics</b> <b>(Concluded)</b>	
Signal Processor Subsystem	
Clutter Canceller	Infinite Impulse Response Design
Suppression	30 dB to 50 dB
Notch half widths	0 to 4 ms <sup>-1</sup> (0 to 8 kts)
Intensity bias	0 to 1 dB
Minimum usable velocity	0 to 4 ms <sup>-1</sup> (0 to 8 kts)
Range increment	0.25 km (0.13 nm)
Azimuth increment	1°
Velocity Calculation	Complex Covariance Argument
Algorithm	Pulse-pair processing
Estimate accuracy (nominal)	1 ms <sup>-1</sup> (2 kts)
Number of pulses averaged	40 to 280
Range increment	0.25 km (0.13 nm)
Azimuth increment	1°
Spectrum Width Calculation	Autocorrelation
Algorithm	Single lag correlation
Estimate accuracy (nominal)	1 ms <sup>-1</sup> (2 kts)
Number of pulses averaged	40 to 280
Range increment	0.25 km (0.13 nm)
Azimuth increment	
Intensity Calculation	Return Power Average
Algorithm	Linear average
Estimate accuracy (nominal)	1 dB
Number of pulses averaged	6 to 64
Range increment	1 km (0.54 nm)
Azimuth increment	1°

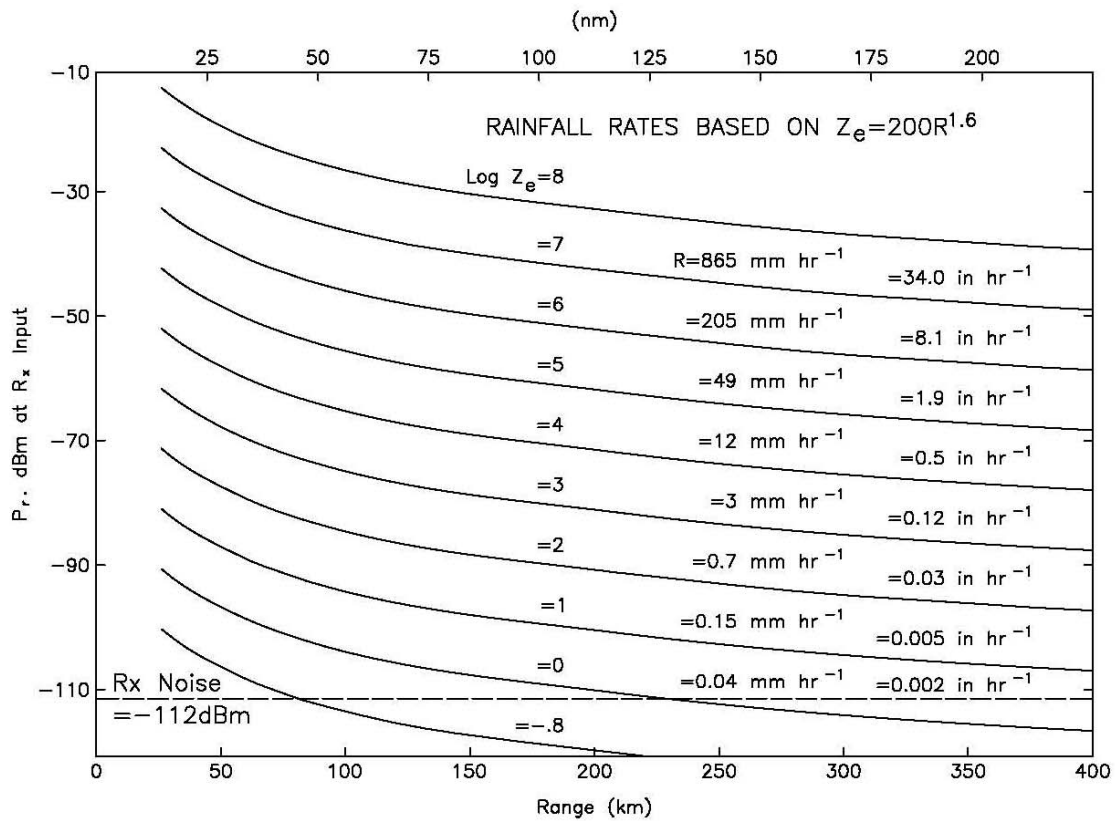


**Figure 2-1**  
**Reflectivity Detection Capability of the WSR-88D**

The equivalent reflectivity,  $Z_e$ , rainfall rate relationship of  $Z_e = 200R^{1.6}$  is a good general relationship, but is not optimum for all types of liquid precipitation and is not valid for snow.

**2.4 Fundamental Concepts of Doppler Radar.** A pulse Doppler radar, in its simplest form, is one providing a signal reference by which changes in the radio frequency (rf) phase of successively received pulses may be recognized. Such a radar is termed "coherent," i.e., it maintains rf waves with a continuous relationship among phases. The known phase of the transmitted signal enables measurement of the phase of the received signal. The Doppler shift associated with the echo from which the return originated is calculated from the time rate of change of phase.

**2.4.1 Doppler Frequency.** The relationship between phase time rate of change and Doppler frequency can be visualized by considering the returned signal from a single target. The complex signal, i.e., inphase, I, and quadrature, Q, returned from a single target at a radial range,  $r$ , is of the form:

$$I = A \cos \left[ \frac{4\pi r}{\lambda} - \Psi \right]$$

$$Q = A \sin \left[ \frac{4\pi r}{\lambda} - \Psi \right]$$

where:

$A$  = signal amplitude (proportional to target cross-sectional area)

$\lambda$  = radar wavelength

$\frac{4\pi}{\lambda}$  = phase due to range propagation of  $2r$  (to the target and back)

$\Psi$  = initial phase of the transmitter signal

If the range,  $r$ , changes with time (target moving relative to the radar), the argument,  $4\pi r / \lambda - \Psi$ , becomes a function of time. Time rate of change of phase is the angular velocity,  $\omega$ , expressed as:

$$\frac{d}{dt} \left[ \frac{4\pi r(t)}{\lambda} - \Psi \right] = \frac{4\pi}{\lambda} \frac{d[r(t)]}{dt} = \frac{4\pi}{\lambda} v_r = \omega$$

since time rate of change of range  $d[r(t)]/dt$  is radial velocity,  $v_r$ , by definition. Since angular velocity,  $\omega$ , is related to frequency,  $f$ , by  $\omega = 2\pi f$ :

$$2\pi \frac{2v_r}{\lambda} = 2\pi f_d$$

and the Doppler frequency,  $f_d$ , is given by:

$$f_d = \frac{2v_r}{\lambda}$$

The angular rate of change is equal to 20 Hz per meter per second of radial velocity for a radar wavelength of 10 cm.

In summary, the fundamental transformations of meteorological characteristics to radar signal characteristics are: target cross-sectional area becomes proportional to signal power, target radial range becomes proportional to signal phase, and target radial velocity becomes proportional to time rate of phase change.

Thus, estimates of these electrical signal properties provide estimates of the corresponding meteorological properties.

**2.4.2 Range-Velocity Ambiguity.** Pulse radar is intrinsically a "sampled data system" since the measurement is time and space discrete. Time corresponds to the pulse repetition time (PRT) and space to the sample volume depth of the radar. The discrete time sampling results in a coupling between the maximum unambiguous range and the maximum unambiguous velocity associated with the radar and the discrete spatial sampling limits the scale that can be resolved by the radar (Section 3.2).

The maximum unambiguous range,  $r_a$ , i.e., the maximum range to which a transmitted pulse wave can travel and return to the radar before the next pulse is transmitted, is simply:

$$r_a = \frac{c PRT}{2}$$

where  $c$  is the wave propagation constant (speed of light);  $c = 3(10^8) \text{ ms}^{-1}$ . For example, a PRT of 1 millisecond (PRF = 1000 Hz) results in an unambiguous range of 150 km (81 nm).

Discrete time sampling, i.e., sampling at the radar PRT interval, also limits the maximum frequency that can be resolved. The rigor for this is given by the Nyquist Sampling Theorem and is somewhat involved, but the mechanisms and implications can be understood by the following considerations.

The Nyquist frequency,  $f_n$ , is the highest frequency that can be resolved by  $\Delta t$  spaced samples. It is given by  $f_n = 1/(2\Delta t)$  and corresponds to two samples per cycle on a sinusoid of  $f_n$ .

Sampling of frequencies higher than  $f_n$  results in an "aliasing" by which frequencies higher than  $f_n$  appear in the range from zero to  $f_n$ . Sampling of frequencies less than and greater than  $f_n$  is illustrated in Figure 2-2.

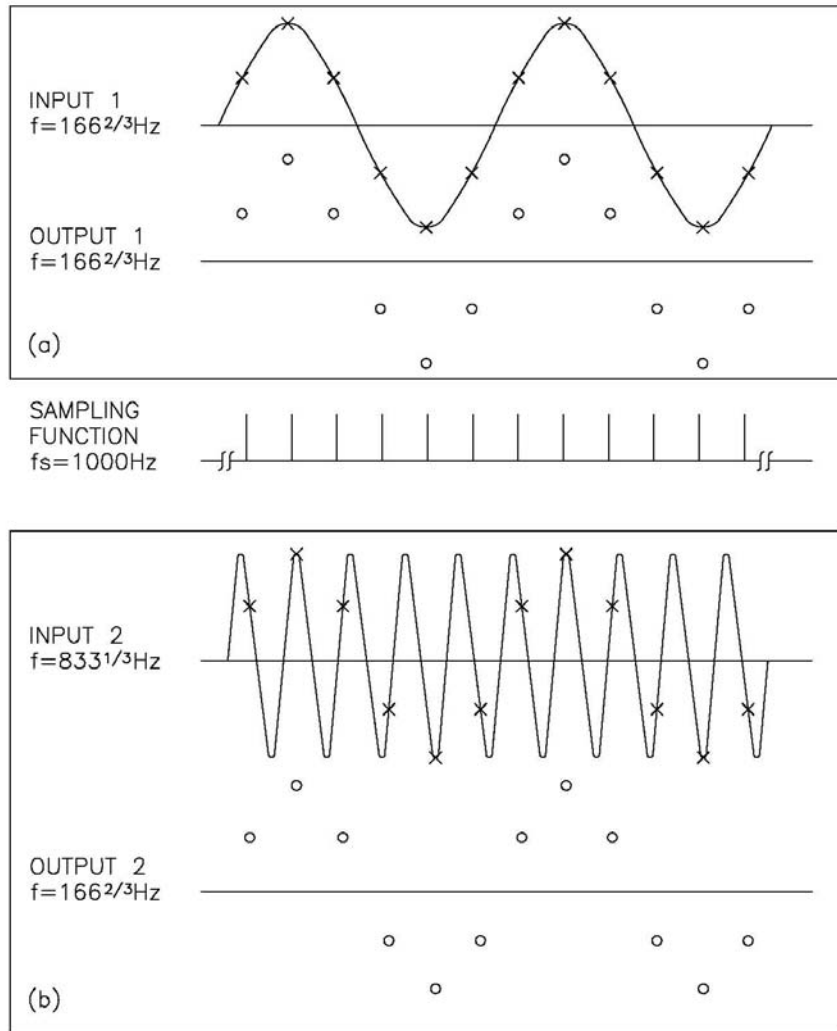


**Figure 2-2**  
**Example of Sampling a Signal**

Input frequency (a) below the Nyquist frequency and (b) above the Nyquist frequency.



Consider the case shown in Figure 2-2a where a frequency of 166 2/3 Hz is sampled every one thousandth of a second (a 1000 Hz rate) and the extrapolated output is a frequency of 166 2/3 Hz, i.e., same frequency as the input. Consider now the case shown in Figure 2-2b where a frequency of 833 1/3 Hz (above the Nyquist frequency) is sampled at a 1000 Hz rate. The extrapolated output frequency is equal to the sampling frequency, 1000 Hz, minus the input frequency of 833 1/3 Hz, which yields a frequency of 166 2/3 Hz.

The limitations on maximum unambiguous frequency,  $f_n$ , imposed by the sampling rate  $f_s = 1/PRT$  results in "coupling" between unambiguous frequency (velocity) and unambiguous range since both are functions of radar PRT. Since:

$$\frac{2 v_a}{\lambda} = f_n = \frac{1}{2} \frac{1}{PRT} \text{ and } r_a = \frac{c PRT}{2}$$

thus,

$$r_a v_a = \frac{c \lambda}{8}$$

where:  $v_a$  = unambiguous velocity  
 $r_a$  = unambiguous range

Thus, the product of unambiguous range and unambiguous velocity is a constant determined by the wavelength of the radar. This relationship is shown in Figure 2-3 for the WSR-88D operating near mid-band. (A detailed discussion is given in Appendix A).

The range-velocity coupling is probably the most important operational constraint of the WSR-88D since it results in the operational problems of range folding and velocity aliasing.

**2.4.3 Velocity Measurement.** The velocity measurement technique used in the WSR-88D is essentially a method of Doppler angular frequency measurement, i.e., measurement of  $\omega = 2\pi f$  in a time-varying function of the form  $y = \cos \omega t$ . This is equivalent to a measure of velocity since frequency is linearly related to velocity by the Doppler equation.

The actual computation is a minimum-variance, unbiased estimation of the complex covariance of the Doppler signal represented by the inphase, I, and quadrature, Q, video signals (a complex signal is needed to measure the sign of the Doppler frequency, i.e., whether the frequency shift is above or below the transmitted signal corresponding to velocities toward or away from the radar).

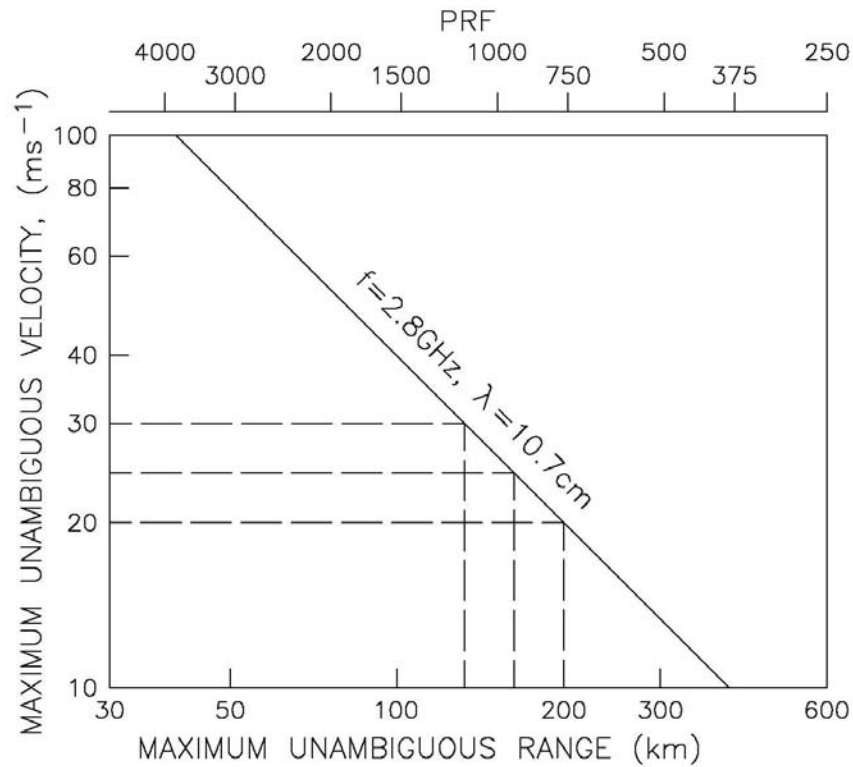


**Figure 2-3**  
**Unambiguous Range-Velocity Relationship for the WSR-88D**

Dashed lines are for unambiguous velocities of 30, 25, and 20  $\text{ms}^{-1}$  with associated unambiguous ranges of 134, 160, and 200 km.

The estimate of velocity ( $v$ ) is:

$$\hat{v} = k \text{ Arg } \sum_{n=1}^{N-1} [Z_{n+1} Z_n^*]$$

where:

$k$  = a constant specified by  $X$  and PRT

$\text{Arg } []$  = the argument or angle of the quantity

$Z$  = a complex signal of the form  $Z = I + jQ$

$Z^*$  = complex conjugate of  $Z$ ,  $Z^* = I - jQ$

$n$  = sample sequence index

$N$  = total number of samples

Due to the discrete nature of the sampling, the angular velocity of the vector represented by  $Z$  is measured as a differential. For example, given the vector  $Z_n = 3 + j3$  in the first quadrant as shown in Figure 2-4a, assume that, by one PRT later, the next sample,  $Z_{n+1} = -4 + j2$ , appears in the second quadrant corresponding to a displacement between samples of 108 degrees. The complex multiplication of the second sample,  $Z_{n+1}$ , and the conjugate of the first  $Z_n^*$  produces a vector ( $Z_{n+1} Z_n^*$ ) magnitude equal to the product of magnitudes of  $Z_n$  and  $Z_{n+1}$  with an angle equal to the difference in angles of  $Z_n$  and  $Z_{n+1}$  or the displacement of the vector over the radar PRT as shown in Figure 2-4b. Angular velocity is thus  $\omega = (\theta_{n+1} - \theta_n)/\text{PRT}$ .

The summation, as shown in Figure 2-4c, produces a mean displacement in which the individual displacements are weighted by the product of the two vector lengths (power of the signal) and the mean velocity is estimated from the power-weighted, average vector displacement.

Using the linear relationship between phase displacement and velocity, Figure 2-4d illustrates what occurs when the input velocity  $v_T$ , corresponding to  $\theta_T$ , exceeds the unambiguous velocity,  $\pm v_a$ , corresponding to  $\pm \pi$ . When the true displacement is greater than  $\pm \pi$ , but less than  $\pm 2\pi$  principal angle detection,  $\theta_m$  corresponds to a measured velocity,  $v_m$ , having a magnitude  $|v_m| = 2v_a - |v_T|$  and with a sign opposite that of  $v_T$ .

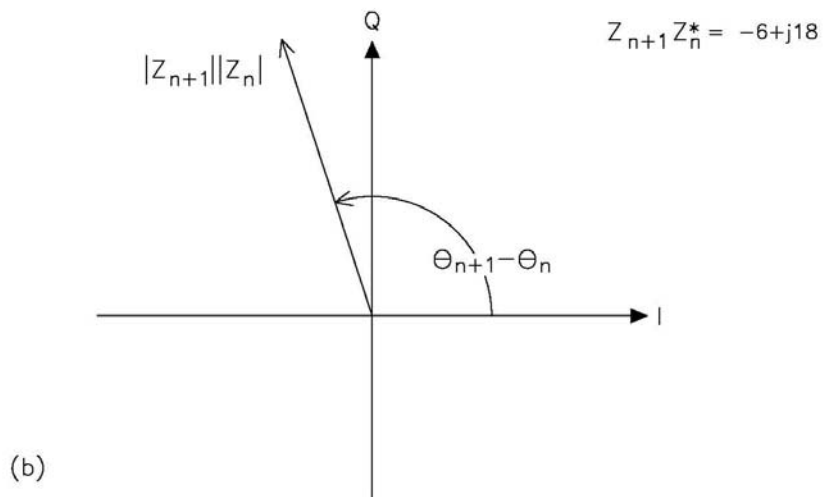
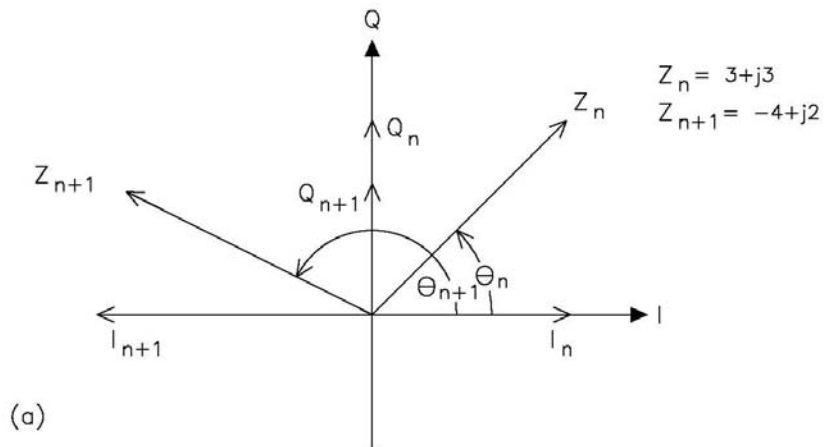


**Figure 2-4**  
**Velocity Sampling**

(a) Vector representation of two consecutive complex video samples ( $I, Q$ ).

(b) Result of the complex multiplication  $Z_{n+1} Z_n^*$

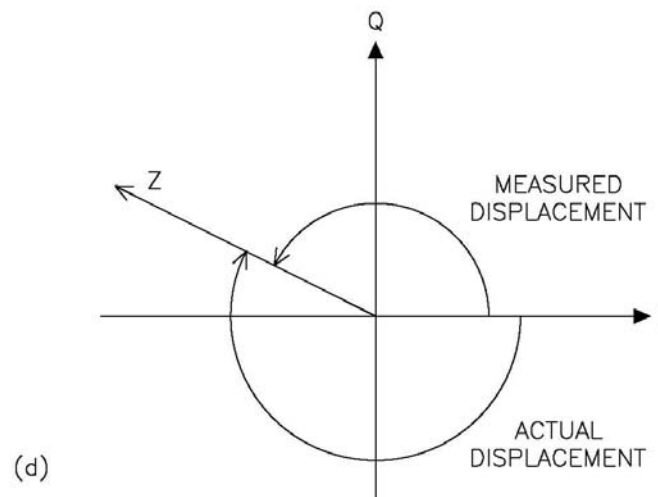
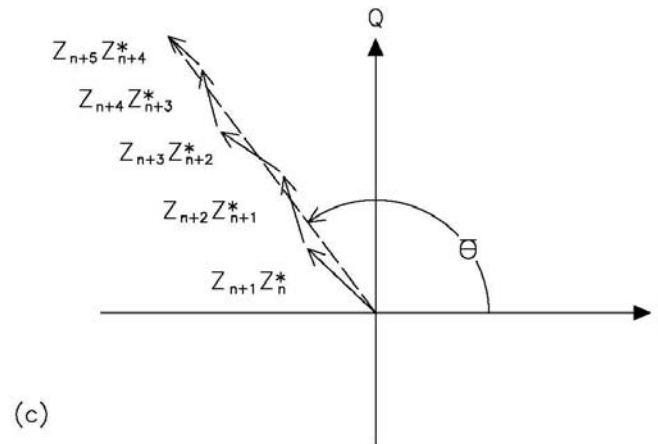


**Figure 2-4  
(Concluded)**

(c) Schematic of vector summation.

(d) Frequency aliasing in the complex plane.

The uncertainty of the velocity estimate, i.e., how well the estimate represents the true mean velocity values, is dependent on input spectrum width--the larger the width the larger the uncertainty. Estimate accuracy can be improved or uncertainty reduced by increasing the number of samples in the estimate. Figure 2-5 gives the estimate accuracy or standard deviation,  $SD[v]$ , (the measured velocity will be within  $\pm$  one standard deviation of the true velocity 63% of the time) as a function of spectrum width with signal-to-noise ratio as the parameter of variation for unambiguous velocities representative of the WSR-88D.

It is seen from Figure 2-5 that the estimate of the standard deviation is dependent on unambiguous velocity,  $v_a$ , input spectrum width,  $W$ , signal-to-noise ratio (SNR), and the square root of the number of samples in the estimate ( $N^{1/2}$ ).

For example, the WSR-88D with wavelength of 10 cm and a pulse repetition frequency (PRF) of 1 kHz [ $v_a = 25 \text{ m s}^{-1}$  (49 kts)], operating at an antenna speed of 3 rpm, delivering estimates on a  $1^\circ$  polar grid (55 samples per estimate), and viewing a meteorological target having spectrum width of  $5 \text{ m s}^{-1}$  (10 kts) at a signal-to-noise ratio of 10 dB delivers a standard error of mean Doppler velocity estimate of  $1 \text{ m s}^{-1}$  (2 kts).

In summary, the mean Doppler velocity estimation technique used on the WSR-88D is a vector calculation of the time rate of change of signal phase that is converted to velocity through radar system constants ( $\lambda$ , PRT). The calculation operates in the continuum of vector space from 0 to  $\pm \pi$  that provides a smooth transition through the Nyquist frequency or maximum unambiguous velocity. Measured velocities,  $v_m$  that are aliased, appear as the difference between the Nyquist co-interval,  $+2v_a$ , and the true velocity,  $v_T$ , i.e.  $v_m = 2v_a - v_T$ . Examination of Figure 2-5 reveals that meteorological parameters influencing estimate standard deviation for a given radar setup are spectrum width and SNR. For a given signal-to-noise ratio, the standard deviation of the velocity estimate increases as the square root of input spectrum width up to widths of about  $0.4v_a$ . At larger spectrum widths, the standard deviation of estimate increases very rapidly (loss of signal coherency) and becomes unacceptable for widths greater than about  $0.5v_a$ . Noise influence on estimate accuracy is negligible for  $SNR > 10 \text{ dB}$ . However, the increase in standard deviation increases very rapidly for  $SNR < 10 \text{ dB}$  and becomes unacceptable in most cases for  $SNR < 0 \text{ dB}$ .

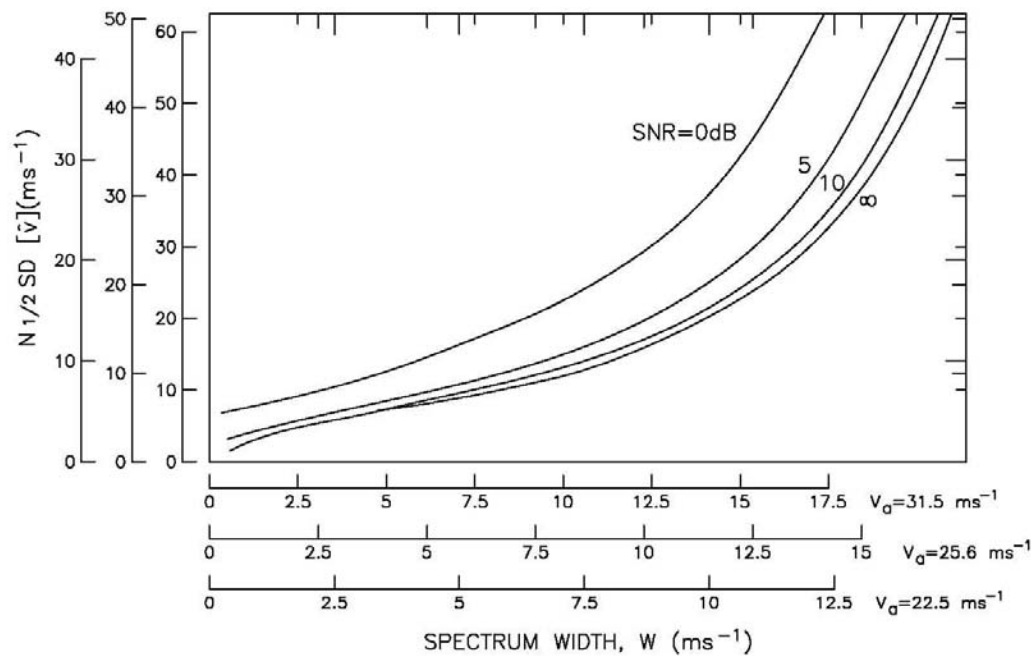


**Figure 2-5**  
**Standard Deviation of the Mean Velocity Estimate**

This figure depicts the normalized standard deviation of the mean velocity estimate as a function of spectrum width for three unambiguous velocities and four levels of signal-to-noise ratio (SNR). Note the ordinate value must be divided by  $N^{1/2}$ , the square root of the number of samples in the estimate.

## REFERENCES

- Miller, K. S., and M. M. Rochwarger, 1972: A covariance approach to spectral moment estimation. *IEEE Transactions on Information Theory*, **IT-18**, No. 5.
- Sirmans D., 1975: Estimation of spectral density mean and variance by covariance argument techniques. Preprints, *16th Conference on Radar Meteorology*, Houston, TX, Amer. Meteor. Soc., 6-13.
- Sirmans, D., and R. J. Doviak, 1973: Meteorological Radar Signal Intensity Estimation. NOAA Technical Memoranda, ERL, NSSL-64, 80 pp.
- Sirmans, D., and B. Bumgamer, 1975: A numerical comparison of five mean frequency estimations. *J. Appl. Meteor.*, **14**, 991-1003.